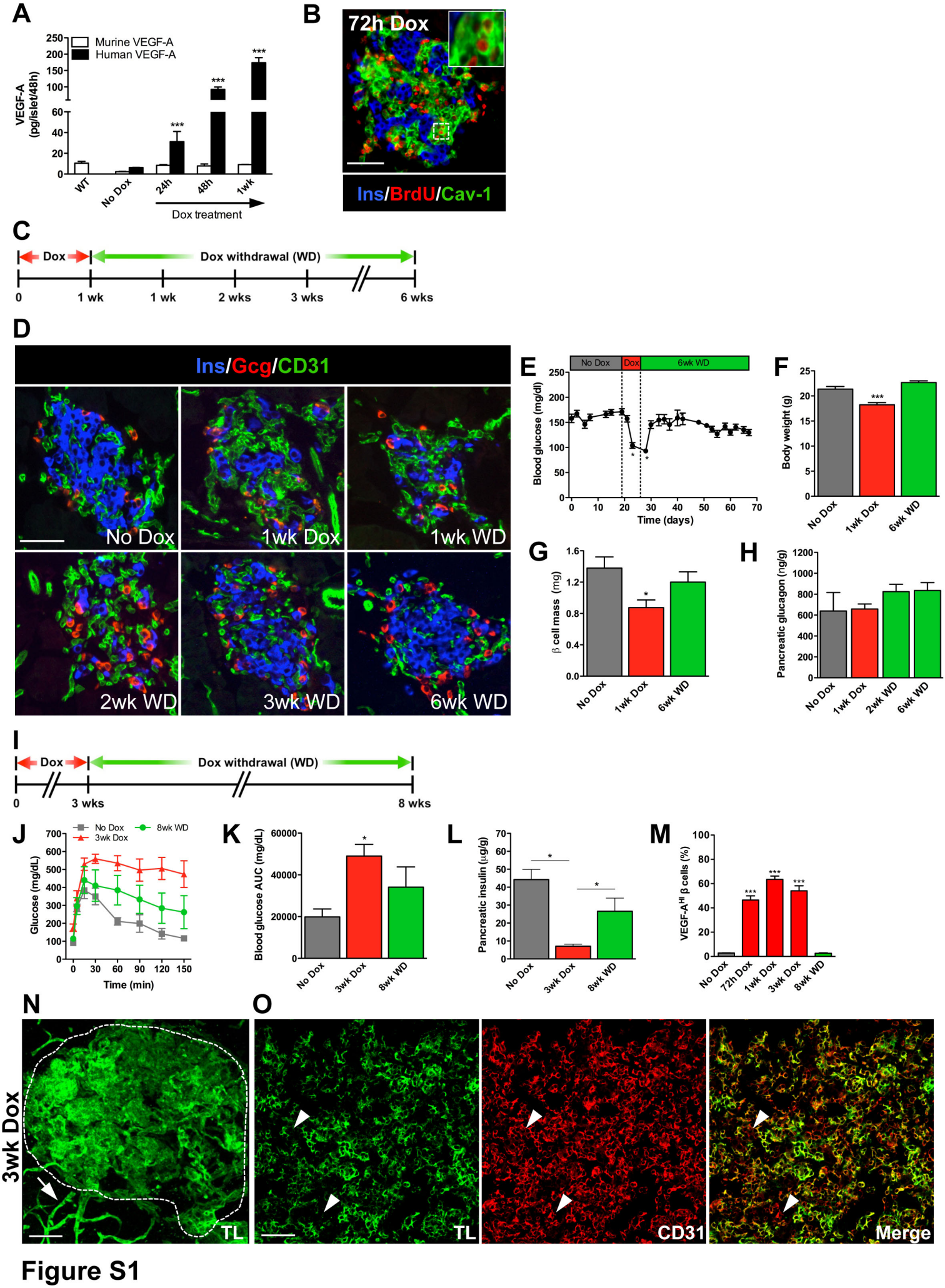
A
Murine VEGF-A
Human VEGF-A
VEGF-A (pg/islet/48h)
WT
No Dox
24h
48h
1wk
Dox treatment
B
72h Dox
Ins/BrdU/Cav-1
C
Dox
Dox withdrawal (WD)
0
1 wk
1 wk
2 wks
3 wks
6 wks
D
Ins/Gcg/CD31
No Dox
1wk Dox
1wk WD
2wk WD
3wk WD
6wk WD
E
No Dox
Dox
6wk WD
Blood glucose (mg/dl)
Time (days)
F
Body weight (g)
No Dox
1wk Dox
6wk WD
G
β cell mass (mg)
No Dox
1wk Dox
6wk WD
H
Pancreatic glucagon (ng/g)
No Dox
1wk Dox
2wk WD
6wk WD
I
Dox
Dox withdrawal (WD)
0
3 wks
8 wks
J
No Dox
3wk Dox
8wk WD
Glucose (mg/dL)
Time (min)
K
Blood glucose AUC (mg/dL)
No Dox
3wk Dox
8wk WD
L
Pancreatic insulin (μg/g)
No Dox
3wk Dox
8wk WD
M
VEGF-A^HI β cells (%)
No Dox
72h Dox
1wk Dox
3wk Dox
8wk WD
N
3wk Dox
TL
O
TL
CD31
Merge

Figure S1

A

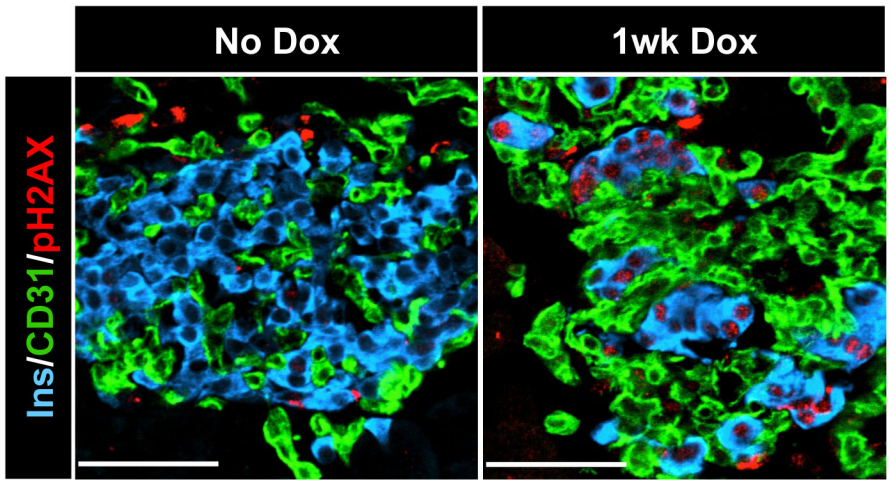
No Dox
1wk Dox
Ins/CD31/pH2AX

B

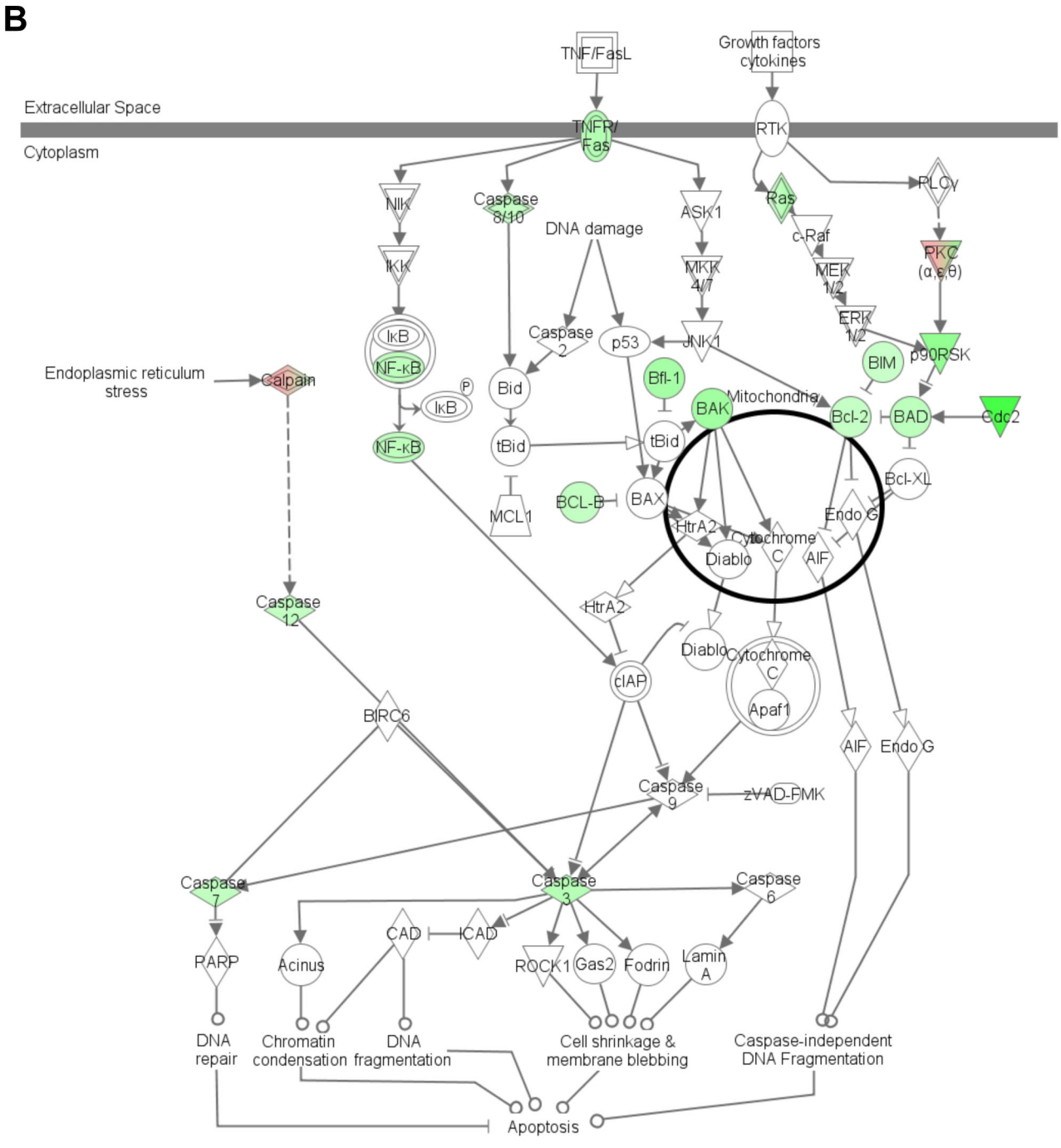
TNF/FasL
Growth factors cytokines
Extracellular Space
Cytoplasm
TNFR/ Fas
RTK
Nik
Caspase 8/10
DNA damage
ASK1
Ras
PLCγ
c-Raf
IKK
MKK 4/7
MEK 1/2
PKC (α,ε,θ)
ERK 1/2
IκB
NF-κB
Caspase 2
p53
JNK1
BIM
p90RSK
Endoplasmic reticulum stress
Calpain
P
IκB
Bid
Bfl-1
Mitochondria
BAK
Bcl-2
BAD
Cdc2
NF-κB
tBid
tBid
Bcl-XL
MCL1
BCL-B
BAX
HtrA2
Cytochrome C
Diablo
AIF
Endo G
Caspase 12
HtrA2
Diablo
Cytochrome C
cIAP
Apaf1
BIRC6
AIF
Endo G
Caspase 9
zVAD-FMK
Caspase 7
Caspase 3
Caspase 6
PARP
Acinus
CAD
ICAD
ROCK1
Gas2
Fodrin
Lamin A
DNA repair
Chromatin condensation
DNA fragmentation
Cell shrinkage & membrane blebbing
Caspase-independent DNA Fragmentation
Apoptosis

Figure S2

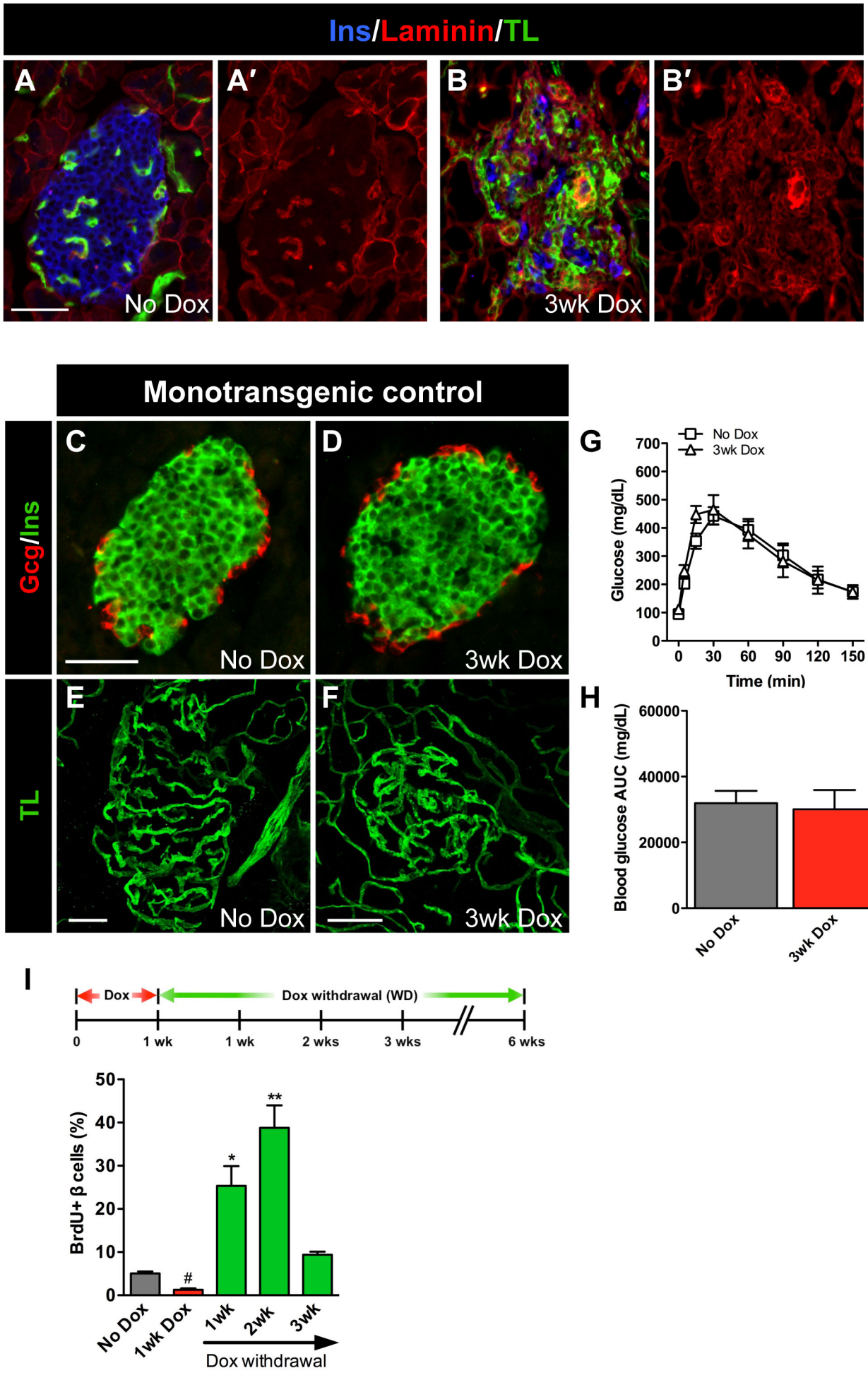
Ins/Laminin/TL
A
A′
B
B′
No Dox
3wk Dox
Monotransgenic control
Gcg/Ins
TL
C
D
E
F
No Dox
3wk Dox
G
No Dox
3wk Dox
Glucose (mg/dL)
Time (min)
H
Blood glucose AUC (mg/dL)
No Dox
3wk Dox
I
Dox
Dox withdrawal (WD)
0
1 wk
1 wk
2 wks
3 wks
6 wks
BrdU+ β cells (%)
No Dox
1wk Dox
1wk
2wk
3wk
Dox withdrawal

Figure S3

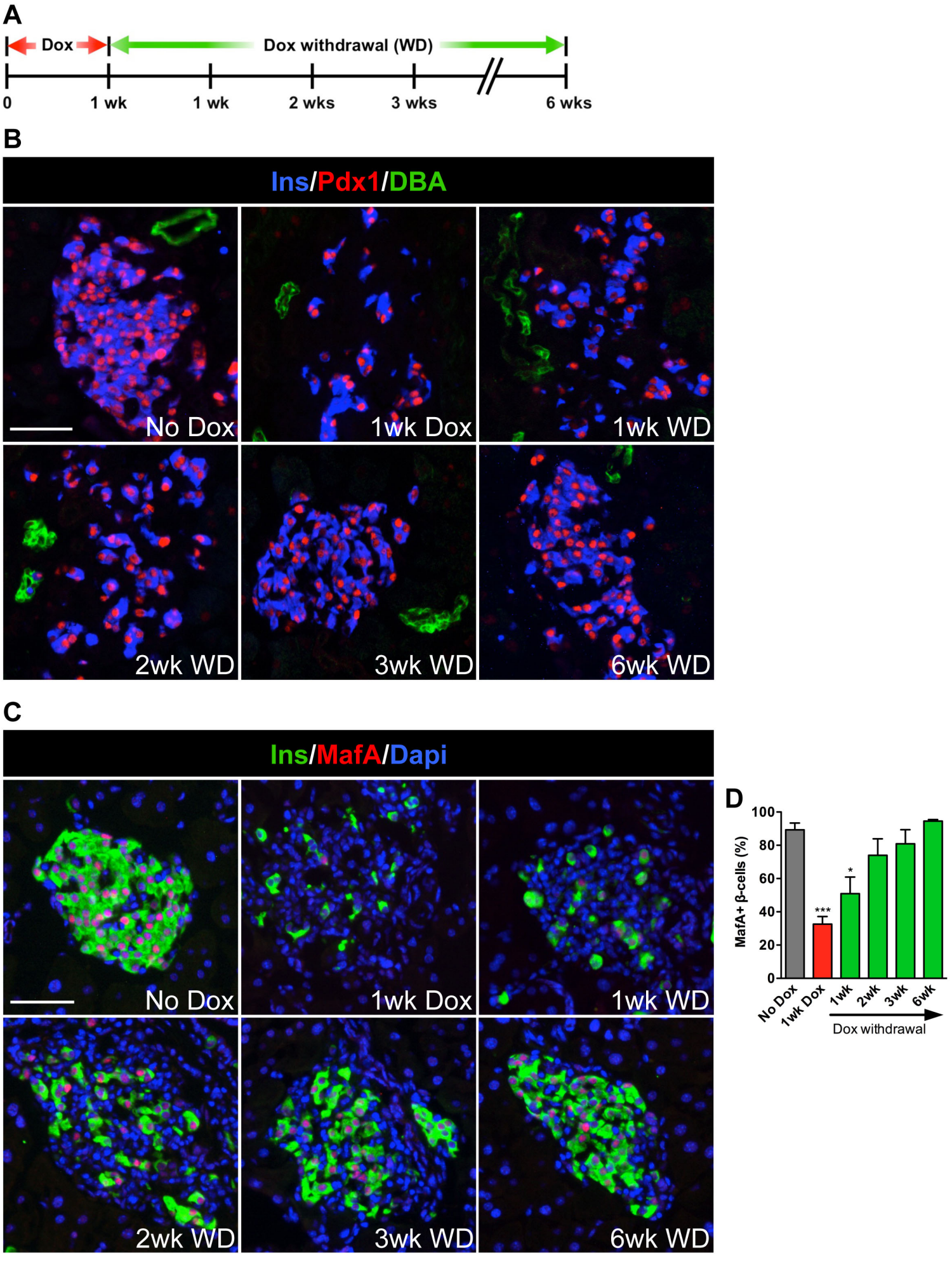
A
Dox
Dox withdrawal (WD)
0
1 wk
1 wk
2 wks
3 wks
6 wks
B
Ins/Pdx1/DBA
No Dox
1wk Dox
1wk WD
2wk WD
3wk WD
6wk WD
C
Ins/MafA/Dapi
No Dox
1wk Dox
1wk WD
2wk WD
3wk WD
6wk WD
D
MafA+ β-cells (%)
100
80
60
40
20
0
***
*
No Dox
1wk Dox
1wk
2wk
3wk
6wk
Dox withdrawal

Figure S4

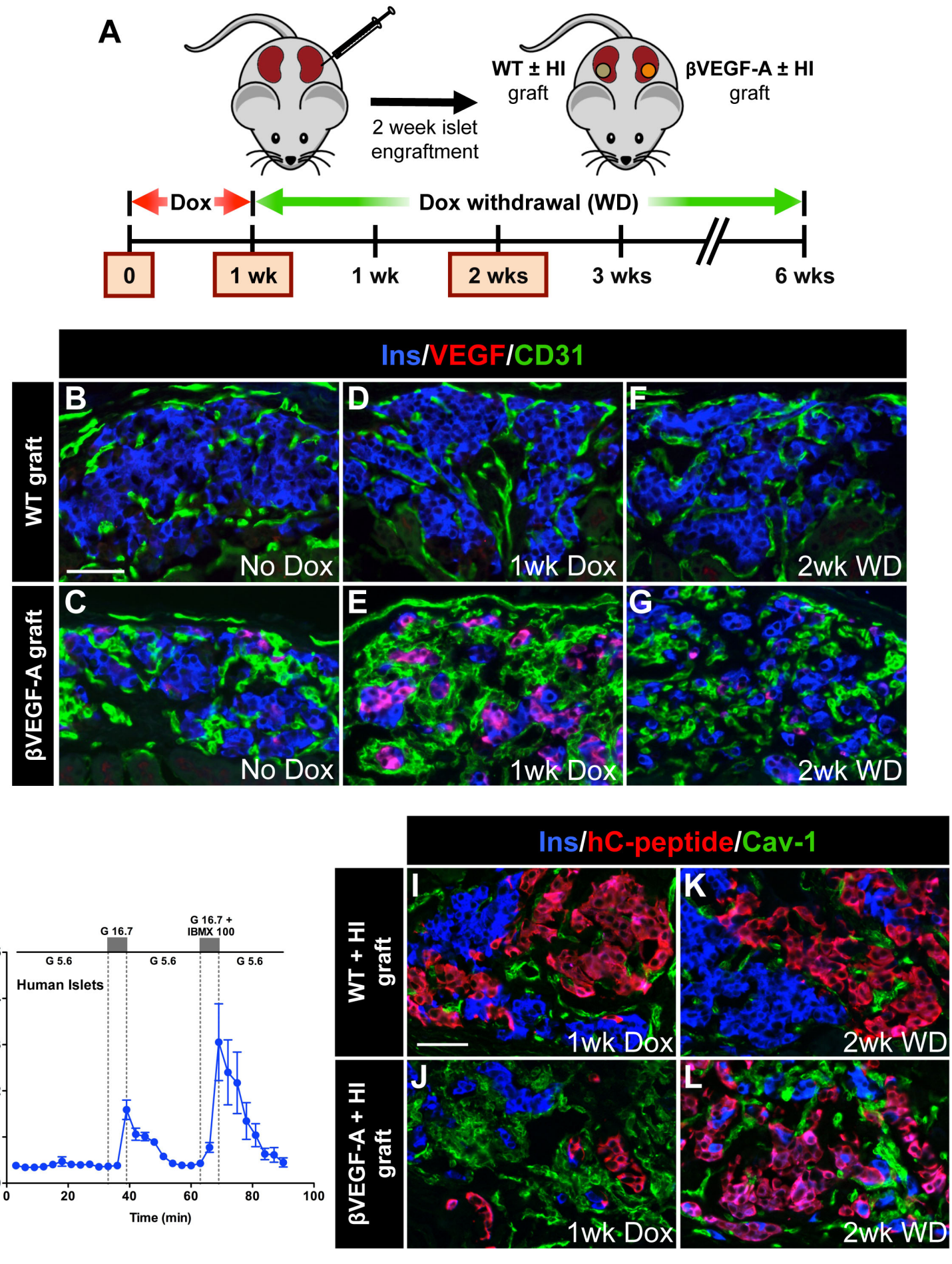
A
WT ± HI graft
βVEGF-A ± HI graft
2 week islet engraftment
Dox
Dox withdrawal (WD)
0
1 wk
1 wk
2 wks
3 wks
6 wks
Ins/VEGF/CD31
WT graft
βVEGF-A graft
B
C
D
E
F
G
No Dox
1wk Dox
2wk WD
H
G 16.7
G 16.7 + IBMX 100
G 5.6
Human Islets
Insulin (ng/100 IEQs/min)
Time (min)
Ins/hC-peptide/Cav-1
WT + HI graft
βVEGF-A + HI graft
I
J
K
L

Figure S5

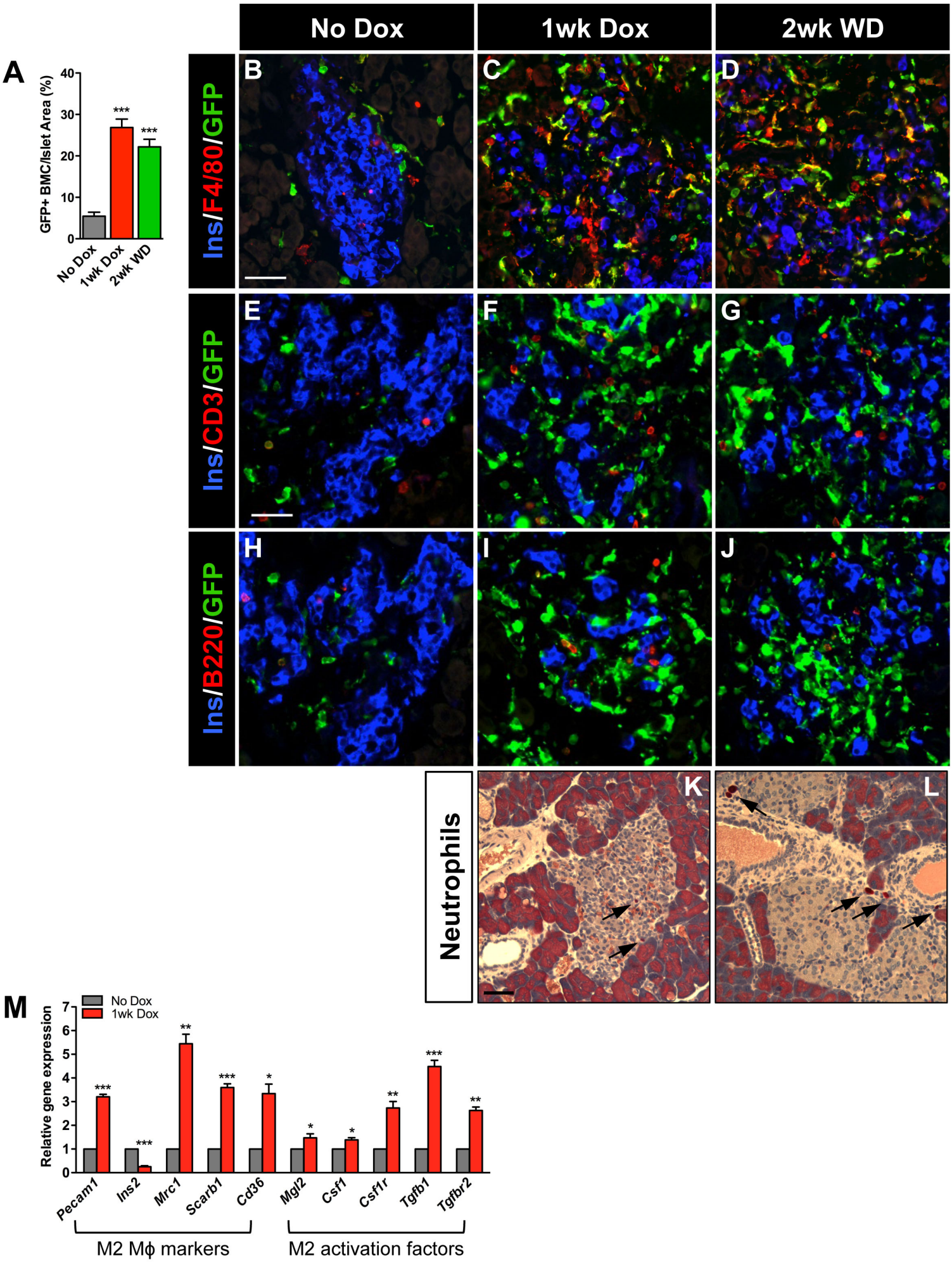
No Dox
1wk Dox
2wk WD
A
GFP+ BMC/Islet Area (%)
40
30
20
10
0
***
***
No Dox
1wk Dox
2wk WD
Ins/F4/80/GFP
Ins/CD3/GFP
Ins/B220/GFP
B
C
D
E
F
G
H
I
J
Neutrophils
K
L
M
No Dox
1wk Dox
Relative gene expression
7
6
5
4
3
2
1
0
Pecam1
Ins2
Mrc1
Scarb1
Cd36
Mgl2
Csf1
Csf1r
Tgfb1
Tgfbr2
M2 Mϕ markers
M2 activation factors

Figure S6

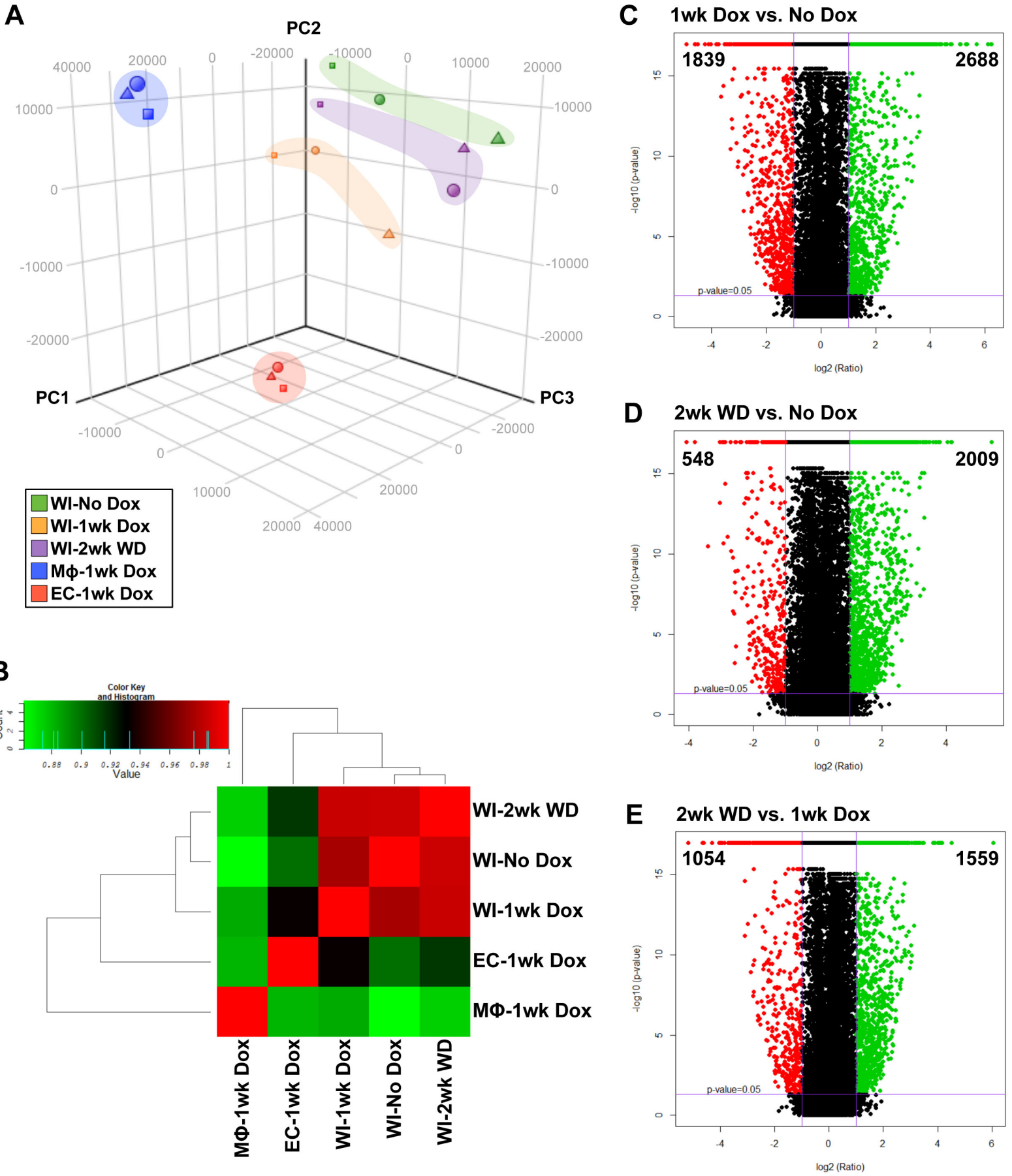
A
PC2
PC1
PC3
WI-No Dox
WI-1wk Dox
WI-2wk WD
Mϕ-1wk Dox
EC-1wk Dox
B
Color Key and Histogram
Count
Value
WI-2wk WD
WI-No Dox
WI-1wk Dox
EC-1wk Dox
MΦ-1wk Dox
C
1wk Dox vs. No Dox
1839
2688
-log10 (p-value)
p-value=0.05
log2 (Ratio)
D
2wk WD vs. No Dox
548
2009
E
2wk WD vs. 1wk Dox
1054
1559

Figure S7

SUPPLEMENTAL FIGURE LEGENDS

Figure S1, related to Figure 1. Phenotypic characterization of βVEGF-A mice after induction and withdrawal of the VEGF-A stimulus. (A) Islet VEGF-A levels increase rapidly after doxycycline (Dox) administration. Levels of murine and human VEGF-A were measured in culture supernatants from isolated WT and βVEGF-A islets prior to and after Dox administration**.** ***, $p<0.001$, human VEGF-A in βVEGF-A islets at 24h Dox, 48h Dox, and 1wk Dox compared with murine VEGF-A in WT and βVEGF-A islets at No Dox, 24h Dox, 48h Dox, and 1wk Dox. (B) Intra-islet ECs undergo extensive proliferation. After 72-hour Dox and BrdU administration, βVEGF-A cryosections were labeled with antibodies to insulin (Ins, blue), BrdU (red), and EC marker caveolin-1 (Cav-1, green). Scale bar in panel B represents 50 μm. Inset shows proliferating ECs in the area denoted by the dashed box. (C-H) Features of the βVEGF-A model after a brief 1-wk Dox administration. (D) Labeling for insulin (Ins, blue), glucagon (Gcg, red), and EC marker CD31 (green). Scale bar in panel D represents 50 μm. (E) Random blood glucose levels; *, $p<0.05$ compared with other time points. (F) Body weight measurements; ***, $p<0.001$, 1wk Dox compared with No Dox or 6wk WD. (G) Pancreatic β cell mass; n=4 mice/time point; *, $p<0.05$, No Dox compared with 1wk Dox. (H) Pancreatic glucagon content, $p=0.3462$; n=5-6 mice/time point. (I-M) Prolonged VEGF-A induction exacerbates the phenotype of βVEGF-A mice. (J, K) Glucose tolerance test in βVEGF-A mice at No Dox (n=7), 3wk Dox (n=7), and 8wk WD (n=6) time points; *, $p<0.05$, 3wk Dox compared with No Dox or 8wk WD. (L) Loss in pancreatic insulin content 3 wks after VEGF-A induction was nearly restored over 8 wks following Dox withdrawal. *, $p<0.05$; **, $p<0.01$; n=3 mice/time point. (M) Assessment of β cells with induced VEGF-A^{HI} expression. ***, $p<0.001$; n=3 mice/time point. (N, O) Blood vessels in βVEGF-A islets remain functional after prolonged βVEGF-A induction. Pancreatic vasculature in βVEGF-A mice was assessed by intravital infusion of endothelium-binding lectin-FITC (TL, green) after 3-wk Dox treatment. (N) Sixty-μm thick pancreatic sections were optically sectioned and 3-D reconstructed. Islet is within the area marked by the dashed line. Arrow points to

normal blood vessels in the adjacent exocrine tissue. Scale bar in panel N represents 50 μm. (O) Ten-μm thick sections of pancreatic tissue labeled intravitally with lectin-FITC (TL, green) were subsequently co-labeled with EC marker CD31 (red). Arrowheads point to CD31+ and TL- EC structures. Scale bar in panel O represents 50 μm.

Figure S2, related to Figures 1 and 2. Transient expansion of intra-islet ECs leads to increased β cell apoptosis. (A) Apoptosis in βVEGF-A islets was examined 1 wk after VEGF-A induction using a marker of DNA double-stranded breaks, gamma-phosphorylated histone H2AX (pH2AX) (Hesse et al., 2009; Lu et al., 2006; Wilson et al., 2011). β cells with nuclear pHA2X labeling were readily detectable after 1 wk Dox, while pHA2X+ β cells were rare prior to VEGF-A induction. Scale bars represent 50 μm. (B) Transcriptome analysis of whole βVEGF-A islets showed increased expression of multiple components of the apoptosis signaling pathway at 1wk Dox compared to No Dox with fold changes >2 (indicated by green color). See Supplemental Experimental Procedures and Figure S7 for transcriptome analysis details.

Figure S3, related to Figures 1 and 2. EC morphology and β cell proliferation in βVEGF-A mice after Dox treatment and effects of Dox on monotransgenic control. (A, B) Capillaries in βVEGF-A islets were assessed at No Dox and 3wk Dox for the basement membrane component laminin; insulin (Ins, blue), laminin (red), and endothelium-binding lectin-FITC (TL, green). Panels A′ and B′ show laminin labeling alone. Scale bar in panel A represents 50 μm and applies to B. (C, D) Cryosections from monotransgenic Tet-O-VEGF-A mice at No Dox and 3wk Dox were labeled with antibodies to insulin (Ins, green) and glucagon (Gcg, red). Scale bar in panel C represents 50 μm and also applies to D. (E, F) Pancreatic vasculature in Tet-O-VEGF-A islets was assessed by intravital infusion of endothelium-binding lectin-FITC (TL, green) at No Dox and 3wk Dox. Scale bars in E and F represent 50 μm. (G, H) Monotransgenic Tet-O-VEGF-A mice treated with Dox for 3 wks maintained normal glucose clearance and

fasting glucose levels. (I) BrdU was administered in drinking water for 1 wk prior to tissue collection. β cell proliferation was assessed in pancreatic cryosections using double immunolabeling with antibodies to insulin and BrdU; n=2 mice/time point. *, $p<0.05$, 1wk WD compared with No Dox, 1wk Dox, or 3wk WD. **, $p<0.01$, 2wk WD compared with No Dox, 1wk Dox, or 3wk WD.

Figure S4, related to Figure 3. Expression of Pdx1 and MafA in βVEGF-A pancreas following induction and withdrawal of the VEGF-A stimulus. (A) Schematic of the experimental timeline. (B) Pancreatic sections from βVEGF-A mice were labeled with antibodies to insulin (Ins, blue), Pdx1 (red), and ductal marker DBA (green). (C) Pancreatic sections from βVEGF-A mice were labeled with antibodies to insulin (Ins, green), MafA (red), and counterstained with Dapi (blue). Scale bars in panels B and C represent 50 μm. (D) Quantification of MafA expression; ***, $p<0.001$, 1wk Dox compared with No Dox, 2wk WD, 3wk WD, or 6wk WD. *, $p<0.05$, 1wk WD compared with No Dox, 2wk WD, 3wk WD, or 6wk WD.

Figure S5, related to Figure 4. Morphology of βVEGF-A islet grafts. (A) Islets from βVEGF-A mice and WT controls were transplanted into βVEGF-A recipients or mixed with human islets (HI) and transplanted into NOD-*scid*-*IL2rγ*^{null} mice. Islets were allowed to engraft for 2 wks then grafts were harvested and analyzed at No Dox, 1wk Dox, and 2wk WD time points; n=3-4 mice/time point (B-G) Cryosections from WT and βVEGF-A grafts were labeled with antibodies to insulin (Ins, blue), VEGF-A (red) and EC marker CD31 (green). Scale bar in panel B is 50 μm and also applies to C-G. (H) Human islets (HI) used in grafts have a robust glucose stimulated insulin secretory response; n=3. (I-L) Cryosections from WT+HI and βVEGF-A+HI grafts were labeled with antibodies to insulin (Ins, blue), human C-peptide (hC-peptide, red) and EC marker caveolin-1 (Cav-1, green). Human β cells co-label with Ins and hC-peptide (purple). Scale bar in panel I is 50 μm and also applies to K-L.

Figure S6, related to Figures 5 and 6. Recruited MΦs infiltrate βVEGF-A islets upon VEGF-A induction, while T cells, B cells, and neutrophils are rare in the infiltrating BMC population. The schematic of the experimental outline is shown in Figure 5. βVEGF-A mice were transplanted with GFP+ bone marrow and 8 wks after bone marrow engraftment VEGF-A was induced transiently by 1-wk Dox administration followed by 2 wks of Dox withdrawal; n=3-4 mice/time point. (A) Quantification of BMC infiltration into βVEGF-A islets at No Dox, 1wk Dox, and 2wk WD time points. ***, $p<0.001$, 1wk Dox and 2wk WD compared with No Dox. Pancreatic cryosections from βVEGF-A mice transplanted with GFP+ bone marrow were analyzed for (B-D) MΦs with antibodies to insulin (Ins, blue), MΦ marker F4/80 (red) and GFP (green); (E-G) T cells with antibodies to insulin (Ins, blue), T cell marker CD3 (red) and GFP (green); and (H-J) B cells with antibodies to insulin (Ins, blue), B cell marker B220 (red) and GFP (green). Scale bar in B is 50 μm and applies to B-D and scale bar in panel E represents 50 μm and applies to panels E-J. (K and L) Paraffin-embedded pancreatic sections from βVEGF mice at 1wk Dox (K) and 2wk WD (L) were analyzed for neutrophils by staining for chloroacetate esterase. Scale bar in panel K represents 50 μm and also applies to panel L. (M) Quantitative RT-PCR analysis of βVEGF-A islets isolated after 1-wk Dox treatment. *, $p<0.05$, **, $p<0.01$, ***, $p<0.001$, 1wk Dox compared with No Dox.

Figure S7, related to Figures 5-7. Transcriptome analysis of βVEGF-A islets and purified islet-derived MΦs and ECs. (A) Principal component analysis (PCA) plot shows the clustering of samples prepared from whole islets (WI, n=3 sets/time point) at No Dox (green), 1wk Dox (orange) and 2wk WD (purple), and purified MΦs (blue, n=3) and ECs (red, n=3) isolated from βVEGF-A islets at 1wk Dox based on their transcriptional profiles. (B) The heat map of the pairwise correlation between all samples based on the Spearman correlation coefficient, which ranks and quantifies the degree of similarity between each pair of samples (perfect correlation=1; red). The highest correlation is between WIs prior to VEGF-A induction (WI-No

Dox) and 2 wks after withdrawal of the VEGF-A stimulus (WI-2wk WD), followed by WIs after VEGF-A induction (WI-1wk Dox). ECs and MΦs after VEGF-A induction (EC- and MΦ-1wk Dox) are most similar to WIs after VEGF-A induction (WI-1wk Dox) and 2 wks after withdrawal of VEGF-A stimulus (WI-2wk WD), when EC and MΦ number are highest in islets. (C-E) Volcano plots display the differential expression of the statistically significant transcripts between βVEGF-A islet samples at No Dox, 1wk Dox, and 2wk WD. Differential expression between conditions was calculated on the basis of fold change (cutoff ≥2.0) and the p-value was estimated by z-score calculations (cutoff 0.05). (C) 1wk Dox vs. No Dox (D) 2wk WD vs. No Dox and (E) 2wk WD vs. 1wk Dox pairwise comparisons. Each volcano plot shows the total number of upregulated (green) and downregulated transcripts (red) in the upper right and left corner, respectively.

SUPPLEMENTAL TABLES

Table S1, related to Figures 1-6. Sources and dilutions of primary antibodies. List of primary antibodies used for immunocytochemistry analysis of pancreatic sections.

Antigen	Species raised	Source	Catalog #	Dilution
Insulin	Guinea pig	Dako	A0564	1:500
Glucagon	Rabbit	Cell Signaling	2760s	1:100
MafA	Rabbit	gift from Dr. Stein	BL1225	1:25000
Pdx1	Rabbit	gift from Dr. Wright	N/A	1:10000
Amylase	Rabbit	Sigma	A8273	1:1000
BrdU	Rat	Abcam	ab6326	1:500
CD31	Rat	BD Pharmigen	550389	1:100
Ki67	Rabbit	Abcam	ab15580	1:500
DBA-biotinylated	N/A	Vector	B-1035	1:1000
CD45	Rat	BD Pharmigen	550539	1:100
B220	Rat	BD Pharmigen	550286	1:100
CD3	Rat	BD Pharmigen	555273	1:100
F4/80	Rat	Invitrogen	MF48000	1:100
GFP	Rabbit	Invitrogen	A11122	1:10000
VEGF-A	Goat	R&D Systems	AF564	1:200
Bmi-1	Mouse	Millipore	05-637	1:200
β-galactosidase	Chicken	Abcam	Ab9361	1:5000
Caveolin-1 (N-20)	Rabbit	Santa Cruz BT	sc-894	1:1000
C-peptide	Mouse	Developmental Studies Hybridoma Bank	GN-ID4-c	1:500
Phospho-histone H2AX (Ser139)	Rabbit	Abcam	ab2893	1:500

N/A-not applicable

Table S2, related to Figures 6 and 7. Sources and dilutions of antibodies for flow cytometry. List of antibodies used for flow cytometry analysis and fluorescence activated cell sorting of MΦs and ECs.

Antigen	Form	Species raised	Source	Catalog #	Dilution
CD45	APC-Cy7	Rat	BD Pharmingen	561037	1:500
CD11b	APC	Rat	BD Pharmingen	561690	1:500
Gr1 (Ly6G/Ly6C)	FITC	Rat	BD Pharmingen	553126	1:500
F4/80	Pacific Blue	Rat	Invitrogen Molecular Probes	MF48028	1:500
CD31	PE	Rat	BD Pharmingen	561073	1:500

Table S3, related to Figure 7. Primers for quantitative RT-PCR. List of primers used for quantitative RT-PCR analysis of βVEGF-A islets isolated after 1-wk Dox treatment.

Gene Symbol	TaqMan Assay ID
Cd36	Mm01135198_m1
Csf1	Mm00432686_m1
Csfr1	Mm01266652_m1
Ins2	Mm00731595_gh
Mgl2	Mm00460844_m1
Mrc1	Mm00485148_m1
Pecam1	Mm01242584_m1
Scarb1	Mm00450234_m1
Tgfb1	Mm01178820_m1
Tgfbr2	Mm00436977_m1
Tbp	Mm00446973_m1

SUPPLEMENTAL EXPERIMENTAL PROCEDURES

Enzyme-linked immunosorbent assay for VEGF-A

Size-matched islets were cultured in eight-well chamber slides containing 50–70 islets/well in 470 µL RPMI-1640 media containing 10% fetal bovine serum and 5.6 mM glucose for 48 hours at 37°C. VEGF-A production by isolated islets was measured by a species–specific VEGF-A enzyme-linked immunosorbent assay (R&D Systems, Minneapolis, MN) as described (Brissova et al., 2006).

Glucose tolerance testing, islet function, and pancreatic hormone content

Intraperitoneal glucose tolerance testing (2 g/kg of body weight) was performed after a 14-16 hour fast (Brissova et al., 2006). Plasma glucose was measured in whole blood using an Accu-chek glucose meter (Roche Diagnostics, Indianapolis, IN) calibrated according to the manufacturer's instructions. Random blood glucose levels were measured at 3:00 pm. Islet function was studied in a dynamic cell perifusion system at a perifusate flow rate of 1 mL/min (Brissova et al., 2006; Wang et al., 1997). The effluent was collected at 3-minute intervals using an automatic fraction collector. Insulin concentration in each fraction was measured by radioimmunoassay (RI-13K, Millipore). Insulin and glucagon content in pancreatic extracts were determined by radioimmunoassay (insulin, RI-13K; glucagon, GL-32K; Millipore).

Tissue collection and immunocytochemistry

Antibodies to all antigens and their working dilutions are listed in Table S1. The antigens were visualized using appropriate secondary antibodies conjugated with Cy2, Cy3, or Cy5 fluorophores from Jackson ImmunoResearch Laboratories, Inc. (West Grove, PA). Secondary antibodies were used at concentrations recommended by the manufacturer. Digital images were acquired with an Olympus BX-41 fluorescence microscope (Olympus, Tokyo, Japan) equipped with a Spot Flex digital camera (Diagnostic Instruments, Inc., Sterling Heights, MI), a Zeiss

LSM510 META laser scanning confocal microscope (Carl Zeiss, Jena, Germany), a Leica DMI6000B fluorescence microscope equipped with a Leica DFC360FX digital camera (Leica, Wetzlar, Germany) or a ScanScope FL (Aperio, Vista, CA). Image analysis was performed using MetaMorph v7.7 software (Molecular Devices, Downingtown, PA) or ImageScope software (Aperio, Vista, CA); 15-20 islets were analyzed/mouse/treatment. A β cell was deemed positive for a nuclear marker only when at least 75% of the nucleus was surrounded by insulin+ cytoplasm; 1000-2000 β cells were assessed/assay/mouse.

BrdU administration and labeling in cryosections

BrdU (Sigma, St. Louis, MO) was administered at 0.8 mg/mL in drinking water for 7 days prior to tissue collection. Cyosections were air-dried, post-fixed with 1% paraformaldehyde/1X PBS for 10 minutes, and permeabilized with 0.5% Triton-X-100/1X PBS for 15 minutes at room temperature. BrdU incorporated into DNA was exposed for immunofluorescence labeling by treatment with DNase (100 Kunitz/mL; Promega, Madison, WI, cat. # M5101-RQ1) in a humidified chamber for 45 minutes at 37°C. The sections were then blocked with 5% normal donkey serum/1X PBS and incubated with primary antibodies to BrdU, insulin and caveolin-1 (Supplemental Table 1) in 0.2% Triton-X-100/1% bovine serum albumin /1X PBS overnight at 4°C. The antigens were visualized using appropriate secondary antibodies conjugated with Cy2, Cy3, or Cy5 fluorophores from Jackson ImmunoResearch Laboratories, Inc. (West Grove, PA). Imaging was performed as described above.

β cell mass measurement

The pancreas was removed, weighed, fixed and then pancreatic cryosections were labeled for insulin and α-amylase. To systematically examine β cell mass in the pancreas, 8-μm pancreatic sections spaced by 200 μm from seven consecutive levels of the pancreatic tissue block were examined (4 pancreata/time point; total of 28 sections/time point). Images of entire pancreatic

sections were captured at 20x magnification using a ScanScope FL system (Aperio, Vista, CA) and archived using a web-based Spectrum digital slide database (Aperio, Vista, CA). Image analysis of whole pancreatic sections was performed with an Aperio area quantification algorithm. β cell mass was calculated by expressing the β cell area (sum of insulin+ area) as a percentage of pancreatic area (combined α-amylase+ and insulin+ area) of the section and then multiplying by the pancreatic weight.

Intravital blood vessel labeling

The function of the islet vasculature was assessed by infusing fluorescein isothiocynate-conjugated tomato lectin (Lycopersicon Esculentum, 1 mg/mL; Vector Laboratories, Burlingame, CA) into the jugular vein as described previously (Brissova et al., 2006).

Islet dispersion and flow cytometry

Islets were isolated as described previously (Brissova et al., 2004) and handpicked in Clonetics EGM MV Microvascular Endothelial Cell Growth Medium (Lonza, Basel, Switzerland). Islets were washed 3 times with 2 mM EDTA/1X PBS and then dispersed by incubating with Accutase (Innovative Cell Technologies, San Diego, CA) at 37°C for 10 minutes with constant pipetting. Accutase was quenched with EGM MV media, and then islet cells were washed twice with the same media and counted using a hemocytometer. Cells were incubated at 4°C with fluorophore-conjugated antibodies in FACS buffer (2 mM EDTA/2% FBS/1X PBS) followed by one wash with FACS buffer. Anti-rat Ig, κ CompBead Plus Compensation Particles (BD Biosciences, San Jose, CA) used for single color compensation controls were also incubated with the appropriate fluorophore-conjugated antibodies. All antibodies for flow cytometry and their working dilutions are listed in Table S2. Prior to analysis or sorting, either propidium iodide (0.05 μg/100,000 cells; Invitrogen Molecular Probes, Eugene, OR) or Dapi (0.25 μg/1,000,000 cells; Invitrogen Molecular Probes, Eugene, OR) was added to samples for non-viable cell exclusion. Flow

analysis was performed using an LSRFortessa cell analyzer (BD Biosciences, San Jose, CA), and a FACSAria III cell sorter (BD Biosciences, San Jose, CA) was used for FACS. Analysis of flow cytometry data was completed using FlowJo 7.6.5 (Tree Star, Ashland, OR).

RNA sequencing and analysis

Isolated whole islets (100-300) or sorted islet-derived cells (50,000-400,000) were added to 200-400 µL lysis/binding solution in the RNAqueous small scale phenol-free total RNA isolation kit (Ambion, Austin, TX). Trace contaminating DNA was removed with TURBO DNA-free (Ambion, Austin, TX). RNA quality control quantification was performed using a Qubit Fluorometer (Invitrogen, Carlsbad, CA) and an Agilent 2100 Bioanalyzer. All RNA samples had an RNA integrity number (RIN) ≥7.0. RNA was amplified using the NuGEN Technologies Ovation RNA amplification kit optimized for RNA sequencing. Following amplification, the resulting cDNA was sheared to an average insert size of 300bp and used for library preparation. Sequencing was performed using standard Illumina methods as described (Malone and Oliver, 2011; Mortazavi et al., 2008). Following RNA sequencing, raw reads were mapped to reference mouse genome mm9 using TopHat v2.0 (Trapnell et al., 2009). Aligned reads were imported onto the Avadis NGS data analysis platform (Strand Scientific Intelligence, Bengalor). Reads were first filtered on their quality metrics, and then duplicate reads were removed. Normalized gene expression was quantified using the TMM (Trimmed Mean of M-values) algorithm (Dillies et al., 2012; Robinson and Oshlack, 2010). The transcriptional profile from each sample group (whole islets at No Dox, 1wk Dox, 2wk WD and sorted islet-derived MΦs and ECs at 1wk Dox) was compared by principle component analysis (PCA) and hierarchal clustering analysis to determine the layout and spread of the samples. Differential expression between conditions was calculated on the basis of fold change (cutoff ≥2.0) and the p-value was estimated by z-score calculations (cutoff 0.05) as determined by the Benjamini Hochberg false discovery rate (FDR) method (Benjamini and Hochberg, 1995). Differentially expressed genes underwent gene set

enrichment analysis (GSEA), gene ontology (GO) analysis, and pathway analysis using DAVID, and Ingenuity Pathway Analysis.

Quantitative RT-PCR

Quantitative RT-PCR was performed on RNA isolated as described above using the primer-probe approach from Applied Biosystems with the primers listed in Table S3. Minimum Information for Publication of Quantitative Real-Time PCR Experiments (MIQE) guidelines were followed for qRT-PCR experiments (Bustin et al., 2009).

SUPPLEMENTAL REFERENCES

Benjamini, Y., and Hochberg, Y. (1995). A direct approach to false discovery rates. J. Royal Stat. Soc., Ser. B *57*, 289–300.

Brissova, M., Fowler, M., Wiebe, P., Shostak, A., Shiota, M., Radhika, A., Lin, P.C., Gannon, M., and Powers, A.C. (2004). Intraislet endothelial cells contribute to revascularization of transplanted pancreatic islets. Diabetes *53*, 1318–1325.

Brissova, M., Shostak, A., Shiota, M., Wiebe, P.O., Poffenberger, G., Kantz, J., Chen, Z., Carr, C., Jerome, W.G., Chen, J., et al. (2006). Pancreatic islet production of vascular endothelial growth factor-A is essential for islet vascularization, revascularization, and function. Diabetes *55*, 2974–2985.

Bustin, S.A., Benes, V., Garson, J.A., Hellemans, J., Huggett, J., Kubista, M., Mueller, R., Nolan, T., Pfaffl, M.W., Shipley, G.L., et al. (2009). The MIQE guidelines: minimum information for publication of quantitative real-time PCR experiments. Clin. Chem. *55*, 611–622.

Dillies, M.-A., Rau, A., Aubert, J., Hennequet-Antier, C., Jeanmougin, M., Servant, N., Keime, C., Marot, G., Castel, D., Estelle, J., et al. (2012). A comprehensive evaluation of normalization methods for Illumina high-throughput RNA sequencing data analysis. Brief. Bioinformatics.

Hesse, J.E., Faulkner, M.F., and Durdik, J.M. (2009). Increase in double-stranded DNA break-related foci in early-stage thymocytes of aged mice. Exp. Gerontol. *44*, 676–684.

Lu, C., Zhu, F., Cho, Y.-Y., Tang, F., Zykova, T., Ma, W.-Y., Bode, A.M., and Dong, Z. (2006). Cell apoptosis: requirement of H2AX in DNA ladder formation, but not for the activation of caspase-3. Mol. Cell *23*, 121–132.

Malone, J.H., and Oliver, B. (2011). Microarrays, deep sequencing and the true measure of the transcriptome. BMC Biol *9*, 34.

Mortazavi, A., Williams, B.A., McCue, K., Schaeffer, L., and Wold, B. (2008). Mapping and quantifying mammalian transcriptomes by RNA-Seq. Nat. Methods *5*, 621–628.

Robinson, M.D., and Oshlack, A. (2010). A scaling normalization method for differential expression analysis of RNA-seq data. Genome Biol. *11*, R25.

Trapnell, C., Pachter, L., and Salzberg, S.L. (2009). TopHat: discovering splice junctions with RNA-Seq. Bioinformatics *25*, 1105–1111.

Wang, T., Lacik, I., Brissova, M., Anilkumar, A.V., Prokop, A., Hunkeler, D., Green, R., Shahrokhi, K., and Powers, A.C. (1997). An encapsulation system for the immunoisolation of pancreatic islets. Nat Biotechnol *15*, 358–362.

Wilson, A.J., Holson, E., Wagner, F., Zhang, Y.-L., Fass, D.M., Haggarty, S.J., Bhaskara, S., Hiebert, S.W., Schreiber, S.L., and Khabele, D. (2011). The DNA damage mark pH2AX differentiates the cytotoxic effects of small molecule HDAC inhibitors in ovarian cancer cells. Cancer Biol. Ther. *12*, 484–493.